Table 1 Eigenvector derivatives of the first nonrigid body mode

$\partial\{\phi\}/\partial p$	Exact	MTM	Error, %	Second order	Error, %	Third order	Error, %
$\partial v_{25}/\partial p$	−0.19963	−0.19156	4.042	−0.19751	1.062	−0.19877	0.431
$\partial v_{26}/\partial p$	−0.25849	−0.26086	0.917	−0.25993	0.569	−0.25902	0.205
$\partial v_{27}/\partial p$	−0.31716	−0.33067	4.260	−0.32004	0.908	−0.31851	0.426
$\partial v_{28}/\partial p$	−0.32978	−0.35281	6.983	−0.33215	0.691	−0.33110	0.400
$\partial v_{29}/\partial p$	−0.33872	−0.36874	8.863	−0.34391	1.532	−0.34058	0.549
$\partial v_{30}/\partial p$	−0.34387	−0.37796	9.914	−0.34897	1.431	−0.34587	0.582
$\partial v_{31}/\partial p$	−0.34516	−0.38018	8.900	−0.35301	2.274	−0.34761	0.710
$\partial v_{32}/\partial p$	−0.34256	−0.37530	9.557	−0.35012	2.467	−0.34603	1.013
$\partial v_{33}/\partial p$	−0.28435	−0.30514	7.311	−0.29219	2.757	−0.28729	1.034
$\partial v_{34}/\partial p$	−0.22664	−0.23613	4.187	−0.22791	0.560	−0.22705	0.181

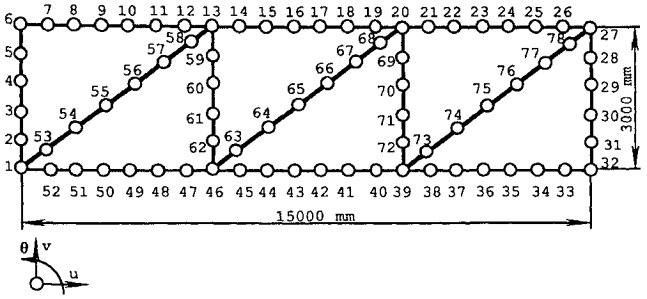

Fig. 1 Plane structure and its finite element mesh.

Numerical Example

To demonstrate its practical applicability, the proposed method has been applied to a structure shown in Fig. 1. The structure was modeled by 83 beam elements with three degree of freedom at each node. Young's modulus is assumed to be $E = 0.75 \times 10^{11}$ N/m^2 and density to be $\rho = 2800$ kg/m^3. The total number of degrees of freedom specified in the finite element model was 234. Without any loss of generality, Young's modulus of element 1 (between nodes 1 and 2) was chosen as design variable p and $\partial[K]/\partial p$ was computed. Since the structure has three rigid body modes, modified similar eigenvalue problem $[[K] + \mu[M]]\{\bar{\phi}\} - \bar{\lambda}[M]\{\bar{\phi}\} = \{0\}$ was solved in which μ was arbitrarily chosen as $0.5\lambda_4$, where λ_4 is the first nonzero eigenvalue of the structure that is $\lambda_4 = 79{,}846(44.97$ Hz). Only the first six ($m = 6$) modes (the first three of them are rigid body modes) were solved, and it is assumed that the eigenvector derivatives of the first nonrigid body modes are of interest. Based on the proposed method, eigenvector derivatives of the first nonrigid body mode were computed, and some of the selected elements (eigenvector elements corresponding to v coordinates at nodes 25–34) are shown in Table 1 together with comparisons with those exact values and those from the mode truncation method (MTM) that is simply the modal method proposed by Fox and Kapoor[2] but with summation up to m available modes instead of all of the N modes of a system. As compared with their exact values, the second order ($k = 0$) and third order ($k = 0, 1$) approximations computed using the proposed method are quite accurate. This demonstrates the usefulness of the proposed method for eigensensitivity analysis of structures with rigid body modes.

Concluding Remarks

A new method for computing eigenvector derivatives of structures with rigid body modes is presented in this Note. The method can be considered as further development of the methods proposed by Wang[4,5] and Liu et al.[6] so that they become generally applicable to any practical structures. Such a generalization requires no extra computational cost yet enables the eigenvector derivatives of structures with rigid body modes to be computed with sufficient accuracy. A numerical example is given to demonstrate the practicality of the proposed method.

References

[1]Haftka, R. T., and Adelman, R. H., "Sensitivity Analysis of Discrete Structural Systems," *AIAA Journal*, Vol. 24, No. 5, 1986, pp. 823–832.

[2]Fox, R. L., and Kapoor, M. P., "Rate of Change of Eigenvalues and Eigenvectors," *AIAA Journal*, Vol. 6, No. 12, 1986, pp. 2426–2429.

[3]Nelson, R. B., "Simplified Calculation of Eigenvector Derivatives," *AIAA Journal*, Vol. 14, No. 9, 1976, pp. 1201–1205.

[4]Wang, B. P., "An Improved Approximate Method for Computing Eigenvector Derivatives," Work-in-Progress Session, AIAA/ASME/ASCE/AHS 26th Structures, Structural Dynamics, and Materials Conf., Orlando, FL, April 1985.

[5]Wang, B. P., "Improved Approximate Methods for Computing Eigenvector Derivatives in Structural Dynamics," *AIAA Journal*, Vol. 29, No. 6, 1991, pp. 1018–1020.

[6]Liu, Z.-S., Chen, S.-H., Min, Y., and Zhao, Y.-Q., "Contribution of the Truncated Modes to Eigenvector Derivatives," *AIAA Journal*, Vol. 32, No. 7, 1994, pp. 1551–1553.

[7]Lin, R. M., "Identification of Dynamic Characteristics of Nonlinear Structures," Ph.D. Thesis, Mechanical Engineering Dept., Imperial College of Science and Technology, London, Jan. 1991.

Parametric Effects on Lift Force of an Airfoil in Unsteady Freestream

Ismet Gursul*
University of Cincinnati, Cincinnati, Ohio 45221
Hank Lin†
University of Southern California, Los Angeles, California 90089
and
Chih-Ming Ho‡
University of California, Los Angeles, Los Angeles, California 90095

Introduction

MANY flows in nature and technology involve cases where the freestream is unsteady. During the forward flight of a helicopter, the freestream velocity varies periodically accompanied by variations in angle of attack. Unsteady airfoils in pitching motion have been reviewed in detail by McCroskey.[1] The purpose of this Note is to report the effects of different operating parameters (reduced frequency, angle of attack, and amplitude of freestream variations) on the lift force of an airfoil in unsteady freestream.

It was shown, in a previous study,[2] that very high lift coefficients are observed depending on the frequency of the freestream variations. Other related studies[3–5] also suggested that other parameters such as angle of attack and amplitude of freestream variations

Received Jan. 30, 1995; revision received July 3, 1995; accepted for publication July 11, 1995.

*Assistant Professor, Department of Mechanical, Industrial, and Nuclear Engineering. Member AIAA.

†Research Assistant, Department of Aerospace Engineering.

‡Professor, Mechanical, Aerospace, and Nuclear Engineering Department. Fellow AIAA.

may be important. Understanding the effect of different parameters may lead to better control of performance. For example, the time-averaged lift force can be increased if the optimum operating conditions are known.

This Note presents the experimental results for a NACA 0012 airfoil. The freestream velocity was varied over a large range of amplitudes and frequencies. Effect of the operating parameters was discussed with the help of flow visualization, velocity, and lift measurements.

Experimental Facility

Experiments were conducted in a vertical unsteady water channel with cross-sectional area of 45.7 × 45.7 cm. The details of the facility and instrumentation can be found in a previous paper.[6] The velocity was measured with a two-component laser Doppler anemometer (LDA) operated in a forward-scattering mode and equipped with a 100-mW argon-ion laser and two LDA counters. The optical system was equipped with a beam expander and Bragg cell for frequency shifting in reversed flows. For the oscillating freestream, the velocity can be represented in the form of

$$U/U_\infty = 1 + R\cos\omega t = 1 + R\cos 2\pi t/T \qquad (1)$$

where U_∞ is the average velocity, R is the dimensionless amplitude ($R < 1$), and $\omega = 2\pi/T$ is the radial frequency.

The chord length of the airfoil was $c = 12.4$ cm, and the Reynolds number based on the chord was about 5×10^4. The blockage ratio was 0.098 for $\alpha = 20$ deg and 0.135 for $\alpha = 30$ deg. A pair of waterproof load cells was used to measure the lift force on the airfoil. No correction was made on lift measurements due to the blockage. The measurement uncertainty for the lift force is 0.5%. The effect of the unsteadiness on the overall performance is best illustrated by considering the average force. For this purpose, a comparison is made with the time-averaged quasisteady lift force, i.e., $\overline{L(t)}/\overline{L_{qs}}$. The quasisteady lift force is defined as

$$L_{qs}(t) = C_{L\infty}\tfrac{1}{2}S\rho U(t)^2 \qquad (2)$$

where $C_{L\infty}$ is the steady-state lift coefficient and S is the surface area of the wing. The main reason for the introduction of the quasisteady force is that it allows for the isolation of the effects due to the unsteadiness.

Results

The previous experiments[2] for $\alpha = 20$ deg showed that the time-averaged lift force is a strong function of the reduced frequency $k = \omega c/2U_\infty$. At an optimum reduced frequency that seems to be independent of amplitude of freestream velocity variations, the time-averaged lift force becomes maximum. In this Note, the effect of the operating parameters is presented from further experiments in the poststall region.

In Fig. 1, the mean lift ratio $\overline{L(t)}/\overline{L_{qs}}$ is shown as a function of the reduced frequency (for $R = 0.29$) for different values of angle of attack in the poststall region. The static stall angle at this Reynolds number is 12 deg. It is seen that there is an optimum reduced frequency for angles of attack larger than the static stall angle, although it is not a sharp peak for $\alpha = 16$ deg. For the static stall angle $\alpha = 12$ deg, there is no optimum reduced frequency.

The optimum reduced frequency is plotted as a function of angle of attack in Fig. 2, which suggests that the optimum reduced frequency is weakly dependent on the angle of attack. The question arises here whether the optimum reduced frequency has any relation to the vortex shedding phenomenon. It should be noted that, for acoustic excitation, the optimum forcing frequency has been found to be the same as the vortex shedding frequency for a stalled airfoil in steady freestream.[7] It is also known that the streamwise oscillations of asymmetric bluff bodies in uniform stream may occur at the natural shedding frequency or its second harmonic (but not at the subharmonic), depending on whether the separated shear layer from leading edge reattaches or not.[8] To investigate any possible relation to natural vortex shedding, spectral analysis of the velocity in the wake of the airfoil in steady freestream was carried out. The variation of the von Kármán vortex street frequency is

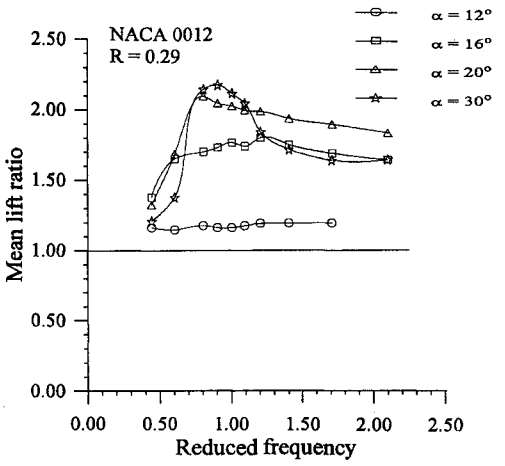

Fig. 1 Variation of time-averaged lift force normalized by time-averaged quasisteady lift force as a function of reduced frequency for several values of angles of attack.

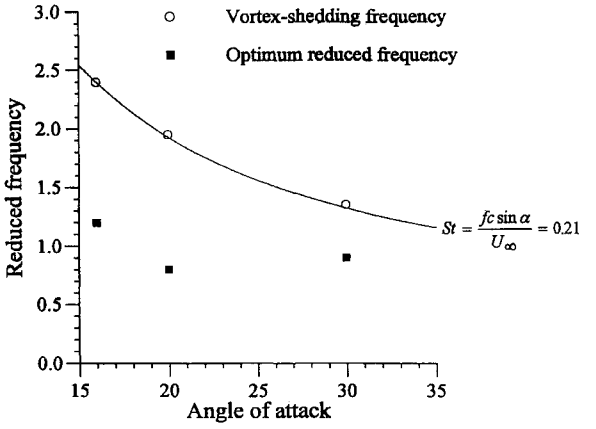

Fig. 2 Variation of optimum reduced frequency as a function of angle of attack.

shown in Fig. 2. These measured values gives a Strouhal number $Sr = fc\sin\alpha/U_\infty = 0.21$, which is in good agreement with the reported values[9] of $Sr \cong 0.19$ for sharp-edged and rounded plates at similar aspect ratios. Clearly, the optimum reduced frequency is not related to the wake instability.

Flow visualization of three cases ($k < k_{opt}$, $k = k_{opt}$, and $k > k_{opt}$) for $R = 0.29$ is shown in Fig. 3. For the optimum case $k = k_{opt}$, the shear layer is already separated from the leading edge at the beginning of the deceleration ($t/T = 0$). During the deceleration, a coherent vortex forms above the wing and becomes very strong in the middle of the cycle when the freestream velocity is minimum ($t/T = 0.5$). For the larger reduced frequency ($k > k_{opt}$), the vortices are smaller in size and it is possible to observe two vortices above the wing. Note that a vortex is located on the wing during the acceleration, which does not permit a complete attached flow as in $k = k_{opt}$. For $k < k_{opt}$, the unsteady effects are not strong and the vortex stays on the wing for a small portion of the cycle. As evidenced by the flow visualization, the scale of the vortice is on the order of chord length when $k = k_{opt}$.

The effect of amplitude for $k = k_{opt}$ was also investigated for an angle of attack $\alpha = 20$ deg. The averaged lift force ($\bar{L}/S\frac{1}{2}\rho U_\infty^2$) was found to increase with amplitude (Fig. 4). In addition to the lift measurements, circulation was calculated from the phase-averaged velocity measurements as a line integral along a (fixed) closed contour around the airfoil. The normalized circulation ($\Gamma/U_\infty c$) varies as a function of time and reaches its maximum value around the middle of the cycle $t/T = 0.5$, when the coherent vortex reaches its climax. Figure 4 shows the variation of the maximum circulation as a function of amplitude R. Both quantities increase with

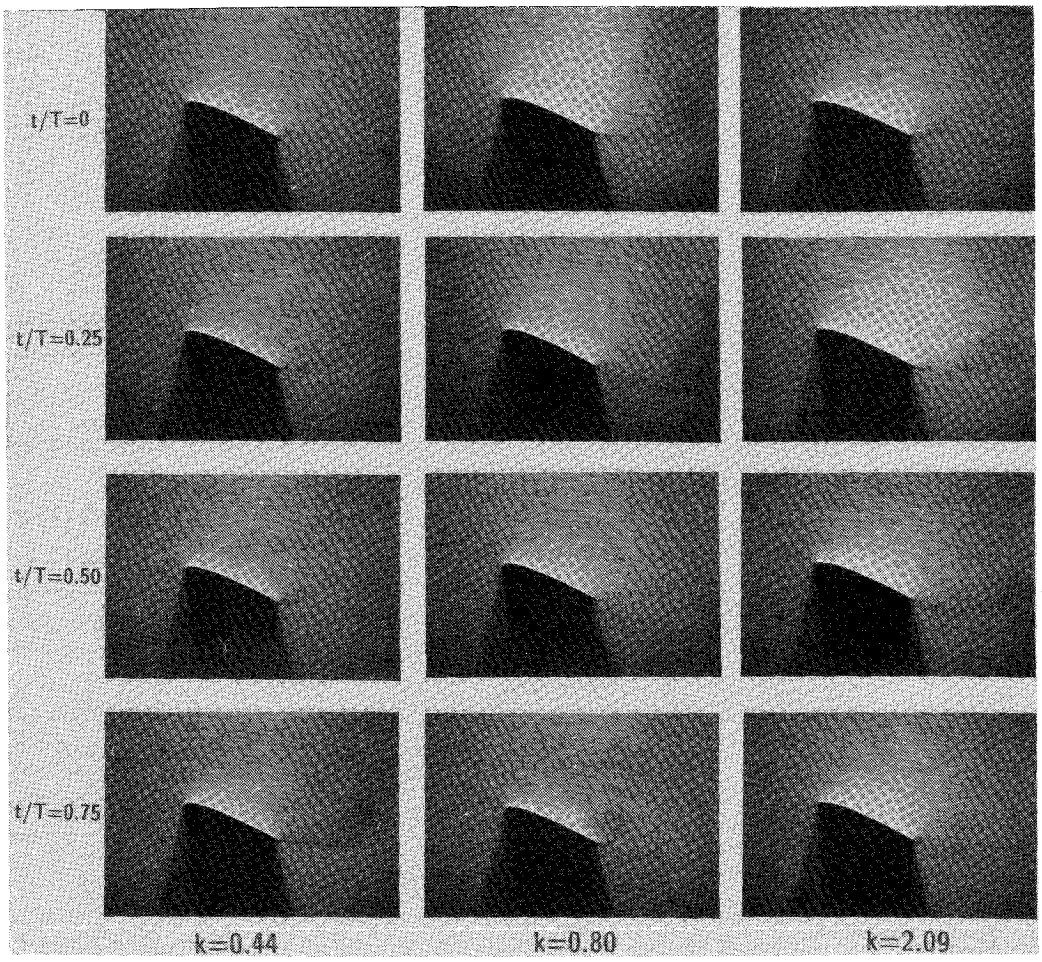

Fig. 3 Flow visualization pictures at several phases during a cycle for different optimum reduced frequencies (R = 0.29).

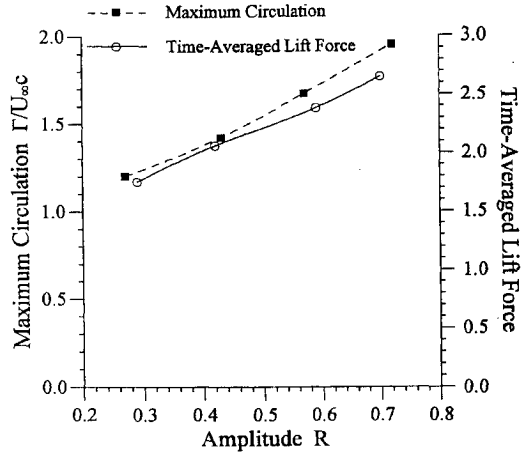

Fig. 4 Effect of amplitude on maximum circulation ($\Gamma/U_\infty c$) and time-averaged lift force ($\bar{L}/S\frac{1}{2}\rho U_\infty^2$) at optimum reduced frequency (α = 20 deg).

the increasing amplitude. It is obvious that the leading-edge vortex makes a major contribution to the overall performance.

Conclusions

The effect of different operating parameters on the lift force of an airfoil in unsteady stream has been investigated. In the post-stall region, there is an optimum reduced frequency at which the time-averaged lift force becomes maximum. The optimum reduced frequency is not related to the wake instability, although the natural vortex shedding frequency and the optimum frequency are on the same order of magnitude. The amplitude of the freestream velocity variation is also a determining parameter for the lift force. The time-averaged lift force increases with increasing amplitude due to the increase in the circulation of the leading-edge vortex.

Acknowledgment

This work was supported by a Contract from the Air Force Office of Scientific Research.

References

[1]McCroskey, W. J., "Unsteady Airfoils," *Annual Review of Fluid Mechanics*, Vol. 14, 1982, pp. 285–311.

[2]Gursul, I., and Ho, C. M., "High Aerodynamic Loads on an Airfoil Submerged in an Unsteady Stream," *AIAA Journal*, Vol. 30, No. 4, 1992, pp. 1117–1119.

[3]Maresca, C., Favier, D., and Rebont, J., "Experiments on an Airfoil at High Angle of Incidence in Longitudinal Oscillations," *Journal of Fluid Mechanics*, Vol. 92, Pt. 4, 1979, pp. 671–690.

[4]Krause, E., and Schweitzer, W.-B., "The Effect of an Oscillatory Freestream-Flow on a NACA-4412 Profile at Large Relative Amplitudes and Low Reynolds-Numbers," *Experiments in Fluids*, Vol. 9, 1990, pp. 159–166.

[5]Shih, C., and Ho, C.-M., "Vorticity Balance and Time Scales of a Two-Dimensional Airfoil in an Unsteady Free Stream," *Physics of Fluids*, Vol. 6, No. 2, 1994, pp. 710–723.

[6]Gursul, I., Lin, H., and Ho, C. M., "Vorticity Dynamics of 2-D and 3-D Wings in Unsteady Free Stream," AIAA Paper 91-0010, Jan. 1991.

[7]Hsiao, F.-B., Shyu, R.-N., and Chang, R. C., "High Angle-of-Attack Airfoil Performance Improvement by Internal Acoustic Excitation," *AIAA Journal*, Vol. 32, No. 3, 1994, pp. 655–657.

[8]Obasaju, E. D., Ermshaus, R., and Naudascher, E., "Vortex-Induced Streamwise Oscillations of a Square-Section Cylinder in a Uniform Stream," *Journal of Fluid Mechanics*, Vol. 213, 1990, pp. 171–189.

[9]Abernathy, F. H., "Flow over an Inclined Plate," *Transactions of the ASME: Journal of Basic Engineering*, Sept. 1962, pp. 380–388.